

ARTICLE

Mounir Traïkia · Dror E. Warschawski
 Michel Recouvreur · Jean Cartaud · Philippe F. Devaux

Formation of unilamellar vesicles by repetitive freeze-thaw cycles: characterization by electron microscopy and ^{31}P -nuclear magnetic resonance

Received: 2 September 1999 / Revised version: 27 February 2000 / Accepted: 27 February 2000

Abstract It has been reported that repetitive freeze-thaw cycles of aqueous suspensions of dioleoylphosphatidylcholine form vesicles with a diameter smaller than 200 nm. We have applied the same treatment to a series of phospholipid suspensions with particular emphasis on dioleoylphosphatidylcholine/dioleoylphosphatidic acid (DOPC/DOPA) mixtures. Freeze-fracture electron microscopy revealed that these unsaturated lipids form unilamellar vesicles after 10 cycles of freeze-thawing. Both electron microscopy and broad-band ^{31}P NMR spectra indicated a disparity of the vesicle sizes with a highest frequency for small unilamellar vesicles (diameters ≤ 30 nm) and a population of larger vesicles with a frequency decreasing exponentially as the diameter increases. From ^{31}P NMR investigations we inferred that the average diameter of DOPC/DOPA vesicles calculated on the basis of an exponential size distribution was of the order of 100 nm after 10 freeze-thaw cycles and only 60 nm after 50 cycles. Fragmentation by repeated freeze-thawing does not have the same efficiency for all lipid mixtures. As found already by others, fragmentation into small vesicles requires the presence of salt and does not take place in pure water. Repetitive freeze-thawing is also efficient to fragment large unilamellar vesicles obtained by filtration. If applied to sonicated DOPC vesicles, freeze-thawing treatment causes fusion of sonicated unilamellar vesicles into larger vesicles only in pure water. These experiments show the usefulness of NMR as a complementary technique to electron

microscopy for size determination of lipid vesicles. The applicability of the freeze-thaw technique to different lipid mixtures confirms that this procedure is a simple way to obtain unilamellar vesicles.

Key words Liposomes · Phosphorus-31 NMR · Large unilamellar vesicles · Freeze-fracture electron microscopy · Dioleoylphosphatidylcholine

Abbreviations *Chol* cholesterol · *DLnPC* dilinoleoylphosphatidylcholine · *DMPA* dimyristoylphosphatidic acid · *DMPC* dimyristoylphosphatidylcholine · *DOPA* dioleoylphosphatidic acid · *DOPC* dioleoylphosphatidylcholine · *DOPG* dioleoylphosphatidylglycerol · *DPPC* dipalmitoylphosphatidylcholine · *EPC* egg phosphatidylcholine · *ESM* egg sphingomyelin · *LPC* lysophosphatidylcholine · *LUV* large unilamellar vesicles · *MLV* multilamellar vesicles · *POPC* 1-palmitoyl-2-oleoylphosphatidylcholine · *SUV* sonicated unilamellar vesicles

Introduction

It is well established that mechanical dispersion of dry lipids in aqueous buffer forms multilamellar vesicles (MLVs) with typical sizes of the order of a micron. Repetitive freeze-thawing cycles are often applied to MLVs in order to homogenize their lipid composition. This procedure also enhances trapping efficiencies due to the breaking of MLVs and the formation of a more homogeneous vesicles population that appears to be largely unilamellar (Mayer et al. 1985). Similarly, freeze-thawing was demonstrated to cause fusion of sonicated unilamellar vesicles (SUVs) (Oku and MacDonald 1983). Fragmentation of dioleoylphosphatidylcholine (DOPC) MLVs into small unilamellar vesicles following freeze-thaw cycles was analyzed in detail by MacDonald et al. (1994). The decrease of the average DOPC vesicle size as a function of number of freeze-thaw cycles was

M. Traïkia · D.E. Warschawski · P.F. Devaux (✉)
 Physico-Chimie Moléculaire des Membranes Biologiques,
 UPR-CNRS 9052, Institut de Biologie Physico-Chimique,
 13 Rue Pierre et Marie Curie, 75005 Paris, France
 e-mail: devaux@ibpc.fr

M. Recouvreur · J. Cartaud
 Biologie Cellulaire des Membranes,
 Institut Jacques Monod,
 UMR 7592, CNRS, Université Paris 6/Paris 7,
 75251 Paris Cedex 05, France

inferred from light absorbance changes and trapping capacity. A more direct determination of the average vesicle size was obtained by electron microscopy and photon correlation spectroscopy and indicated an average diameter of 145 nm after 10 freeze-thawing cycles (MacDonald et al. 1994). However, the latter report did not show the size distribution of the freeze-thawed vesicles. The technique of unilamellar vesicle preparation by freeze-thawing is rather simple and can be used in principle for biotechnical applications (drug encapsulation) or for biophysical investigations on model membranes. It is sometimes complemented by filtration, supposedly to obtain homogeneous vesicle size. Indeed, freeze-thawing does not give a population of vesicles with the same size. Furthermore, fragmentation as well as fusion by repeated freeze-thawing do not have the same efficiency for all lipid mixtures. A precise knowledge of the size distribution would be useful in particular for comparison with other techniques of vesicle preparation such as large unilamellar vesicles (LUVs) produced with an extruder (Hope et al. 1985) or by a reverse phase procedure (Szoka et al. 1980).

Electron microscopy and light scattering are often used to determine vesicle sizes. In this study we demonstrate that ^{31}P NMR can be a very powerful technique for this purpose. The fragmentation of lipid vesicles modifies NMR lineshapes because of the change in averaging of the anisotropic chemical shift and relaxation parameters of the phosphorus nuclei (Dufourc et al. 1992). Thus, one can take advantage of the change in lineshape of ^{31}P NMR spectra to monitor the change in size distribution of different phospholipid mixtures upon repeated freeze-thawing. We show that analysis of NMR spectra provides an estimate of the size distribution profile probably more accurate than statistical analysis of freeze-fracture or negative staining electron micrographs.

Materials and methods

Chemicals

Egg phosphatidylcholine (EPC), egg sphingomyelin (ESM), DOPC, 1-palmitoyl-2-oleoylphosphatidylcholine (POPC), dimyristoylphosphatidic acid (DMPA), dimyristoylphosphatidylcholine (DMPC), dipalmitoylphosphatidylcholine (DPPC), dilinoleoylphosphatidylcholine (DLnPC), dioleoylphosphatidylethanolamine (DOPE), dioleoylphosphatidylglycerol (DOPG), lysophosphatidylcholine (LPC) and cholesterol (Chol) were purchased from Sigma and were used without further purification. Dioleoylphosphatidic acid (DOPA) was obtained from DOPC by hydrolysis of the choline head group using phospholipase D (Roux et al. 1983). The purity of all lipids was verified by thin layer chromatography and by high-resolution NMR in

chloroform. Deuterium oxide (D_2O) was obtained from Eurisotop (Saint-Aubin, France), and *N*-(2-hydroxyethyl)piperazine-*N'* (ethanesulfonic acid) (Hepes), ethylenediamine-tertraacetic acid (EDTA) and KCl were purchased from Sigma.

Preparation of freeze-thawed liposomes

MLVs were obtained by mixing phospholipids at the desired ratio in chloroform. Chloroform was removed first at room temperature with a rotary evaporator. Residual organic solvent was removed by pumping for at least 2 h with a mechanical vacuum pump. Either a 1:1 (v/v) mixture of H_2O and D_2O or a 1:1 mixture of D_2O and Hepes buffer (0.1 M Hepes, 0.1 M KCl, 5 mM EDTA, pH 8.0) was added to the lipid film (final concentration for lipid mixtures was 100 mg/mL) and the sample vortexed to emulsify the lipid mixture. The lipids in a 5 mL glass tube were then dipped into liquid nitrogen for rapid cooling. After 3 min, the frozen lipids were transferred to a bath at 60 °C for thawing. After 3 min in the hot bath, the lipids were frozen again. This operation was repeated several times as indicated.

SUVs were prepared by sonication of MLV dispersion under a stream of argon using a probe-type sonicator (model VC50, Bioblock Scientific, Paris) at 40 W in an ice bath until a clear solution was obtained (which required approximately 30 min). The sample was afterwards centrifuged at 11,000g for 15 min to ensure the removal of metallic particles.

LUVs were prepared by the reverse phase evaporation technique (Szoka et al. 1980). The lipid mixture (25 mg total lipid) in chloroform/methanol solution was deposited on the sides of a round-bottom flask by removal of the organic solvent by rotary evaporation. The lipids were then redissolved in 2 mL diethyl ether. Hepes buffer (0.5 mL) was added to the organic solution of phospholipids and the mixture was sonicated in a probe-type sonicator for 2 min. The mixture was placed on a rotary evaporator and the remaining organic solvent was removed under vacuum in two stages: evaporation at 400 mmHg until the suspension became a gel, followed by a brief vortex mixing and then continued evaporation at 730 mmHg until a homogeneous suspension was obtained. The preparation (50 mg/mL for all lipid mixtures) was extruded through 0.4 μm then 0.2 μm polycarbonate membranes.

Electron microscopy

The same vesicles were used for NMR spectroscopy and for electron microscopy except that vesicles (100 mg/mL for all lipid mixtures) were mixed with glycerol (50% v/v) as cryoprotectant and frozen rapidly in a propane

slush for freeze-fracture investigations. Quenched samples were fractured in a Balzers BAF 300 freeze-fracture apparatus (Balzers, Liechtenstein) equipped with an electron beam device for platinum and carbon shadowing and a quartz crystal monitor for regulating shadow thickness (2 nm for platinum and 20 nm for carbon). The replicas were cleaned in sodium chlorate solutions and collected on 300-mesh copper grids coated with collodion film.

The replicas were examined in a Philips CM 12 electron microscope operating at 80 keV. The pictures were taken on Kodak electron microscope films 4489 at nominal initial magnifications of 15,000 \times and 26,000 \times . The size distributions were measured on 2.5 \times magnified prints. Dimensions of the freeze-fractured vesicles were measured as the largest length in the direction perpendicular to the shadowing direction. In the case of unilamellar vesicles, most profiles of the fractured lipid shells were circular and it could therefore be assumed that they were derived from spherical vesicles. As discussed in Heegaard et al. (1990), in the case of an homogeneous population of spherical vesicles with the same diameter D , the effect of non-equatorial fractures introduces a small correcting factor between the weighted mean diameter D_m obtained by assuming a random intersection of identical spheres and the actual diameter D of these spheres. Namely:

$$D_m = (\pi/4)D \quad (1)$$

About 200–1500 vesicles were counted for each sample. Accuracy of size determination was about 10 nm, corresponding to 0.5 mm on the ruler.

For negative staining, vesicle samples (1–10 mg/mL) were diluted in 0.1 M ammonium acetate buffer (pH 7.4) containing 10 μ g/mL bacitracin. Drops of vesicles were deposited onto carbon-coated grids, and negatively stained with 1% aqueous uranyl acetate. Grids were directly observed in the microscope (80 keV). Pictures were taken at a magnification of 15,000 \times under minimal irradiation conditions.

NMR experiments

NMR measurements were performed on a Bruker 400 AMX, wide-bore spectrometer operating at 162 MHz for ^{31}P using a 10 mm liquid probe. Spectra were acquired using a phase cycled Hahn echo with proton broad band decoupling (WALTZ16) (Rance and Byrd 1983). Typical acquisition parameters were: 90 $^\circ$ pulse length 10 μ s; echo delay 40 μ s; recycle delay 3 s or 5 s, after checking that the lineshape is not distorted; spectral width 100 ppm (16 kHz). In all experiments, 16 k complex points were acquired, zero filled to 32 k before Fourier transformation, exponentially multiplied with 50 Hz line broadening, and treated with automatic baseline correction. Each spectrum was the average of 5–18 k scans.

NMR spectral simulation

The effect of vesicle size distribution, polydispersity and multilamellarity can be accounted for in the simulations of ^{31}P NMR spectra by considering both the rotational diffusion of the vesicles and the lateral diffusion of phospholipids along the curved surfaces (Burnell et al. 1980). The tensor representing the chemical shift anisotropy of the phosphate moiety is considered to be axially symmetric due to the rapid motion of the phospholipids around the local normal of the bilayer. Additional averaging is due to phospholipid reorientation caused by vesicle tumbling τ_t or lateral diffusion within each vesicle; the latter reorientation is associated with a characteristic time, τ_{diff} . One can introduce an effective characteristic time τ , defined by the following expression:

$$\frac{1}{\tau} = \frac{1}{\tau_t} + \frac{1}{\tau_{\text{diff}}} = \frac{6}{r^2}(D_t + D_{\text{diff}}) \quad (2)$$

where $D_t = kT/8\pi r\eta$ is the rotational diffusion coefficient of the vesicles, η being the viscosity of the medium. The simulation program employed in the present study was inspired from the doctorate thesis of Rance (1981) as developed in Douliez et al. (1994). We have modified the program in order to include the isotropic chemical shift of each lipid in lipid mixtures and to allow us to test particular size distribution profiles. The following values were used in the simulations: $T = 298$ K; $D_{\text{diff}} = 10^{-7}$ cm 2 /s (Galla et al. 1979) and $\eta = 7.808 \times 10^{-4}$ Poise.

Frequency shifts were referred to the isotropic chemical shift of DOPC. The overall chemical shift anisotropy ($\Delta\sigma$) in the absence of averaging by vesicle tumbling and/or lateral diffusion was obtained from the difference between parallel and perpendicular chemical shifts as measured on the NMR spectrum recorded with MLVs in the fluid state before freeze-thawing. The isotropic chemical shifts of LPC, DOPE and DOPG were determined in SUVs and corresponded to low-field shifts of $\delta_{\text{iso}} = 0.5$ ppm, 0.6 ppm and 1.1 ppm, respectively. For DOPA, δ_{iso} was in the range 2–3 ppm, towards low fields. This value is strongly dependent upon pH, temperature and ionic strength (Swairjo et al. 1994; Traïkia et al. 1997). For lipid mixtures, $\Delta\sigma$ can be evaluated for each lipid by measuring the distance between the high field peak ($\theta = 90^\circ$) which is always clearly visible, and the theoretical position of the isotropic peak, δ_{iso} of the corresponding lipid. We found $\Delta\sigma = 45 \pm 1$ ppm for DOPC, DOPG, EPC, POPC, DMPC, DPPC and DLnPC. The same value was obtained for DOPA under our conditions of pH and temperature. When LPC was incorporated in DOPC vesicles, two powder patterns were observed and revealed that LPC had a significantly smaller chemical shift anisotropy, with $\Delta\sigma = 35 \pm 1$ ppm.

The intrinsic linewidth, which is proportional to $1/T_2$, is theoretically orientation dependent for ^{31}P NMR. Smith and Ekiel (1984) have reported the following values for phospholipids in MLVs: $T_2 = 2.4$ ms for

$\theta = 0$ and $T_2 = 7.4$ ms for $\theta = \pi/2$, where θ is the angle between the normal to the bilayer and the direction of the magnetic field. In our simulations the lorentzian linewidth, $\Delta\nu$, was calculated for each orientation by using Seelig's formula (Seelig 1978):

$$\Delta\nu = \frac{1}{\pi T_2} = R_1 + R_2(3 \cos^2 \theta - 1)$$

where R_1 and R_2 are adjustable parameters; R_1 can be determined in systems where the anisotropy is averaged out. DOPC has a linewidth in Triton X100 around 30 Hz and in SUVs in the range 40–50 Hz. In SUVs made with DOPC/DOPA, the DOPA linewidth is always found larger than that of DOPC. It is also a function of the pH and of the packing imposed by the curvature, which is different for the inner and outer leaflets (Swairjo et al. 1994). In practice, R_1 values were adjusted in the range 20–100 Hz for DOPC, DOPG and LPC while R_1 was selected in the range 100–500 Hz for DOPA. An optimum value for R_2 was 600 Hz. This value was fixed in all the simulations.

It can be assumed that all lamellae of a given MLV have the same tumbling rate, which depends only on the radius of curvature of the most external bilayer. On the other hand, the reorientation of the phospholipids by lateral diffusion depends upon the actual radius of each individual vesicle within one MLV. Thus ^{31}P NMR spectra of MLVs can be simulated: (1) by assuming a fixed external radius and a variable number of inner bilayers, or (2) by assuming that the number of inner bilayers is determined by a periodic spacing between lamellae, the smaller vesicle possessing an arbitrary diameter of 20 or 30 nm, while the external diameter is variable (Douliez et al. 1994). Obviously, if the number of lamellae and the external radius are allowed to vary for the same sample, there are too many parameters to reach unambiguous conclusions. For that reason the lamellarity was determined independently by electron microscopy freeze-fracture studies.

For spectra corresponding to a population of unilamellar vesicles, Douliez et al. (1994) assumed a Gaussian distribution. However, in our particular case, optimum fits of the spectra were obtained with a distribution of vesicle diameters, which decreased exponentially from a maximum for small diameters to zero frequency for large diameters.

Results

Freeze-fracture electron microscopy

We have carried out freeze-fracture electron microscopy on various lipid suspensions: DOPC, DOPC/DOPA, DOPC/LPC, DOPC/DOPA/LPC, DOPC/Chol, EPC, DLnPC, DMPC, DPPC, ESM and DMPC/DMPA. Figure 1a–c shows freeze-fracture electron micrographs

of DOPC/DOPA (80:20 mol%) vesicles before and after freeze-thawing, with 0, 10 and 50 cycles, respectively. The multilamellar vesicles become in the majority unilamellar following freeze-thawing, and have a quasi-spherical shape. Quantitative evaluation of the percentage of unilamellar vesicles was achieved by analyzing micrographs obtained with vesicles of different lipid composition obtained after 10 freeze-thaw cycles. The percentage of vesicles remaining multilamellar after fragmentation was practically zero for DOPC/DOPA or DOPC/LPC, about 2% of the vesicles appeared multilamellar in the case of DOPC alone or DOPC/Chol (70:30 mol%) and about 5% in the case of EPC. If less than 10 cycles were used, a larger number of multilamellar vesicles could be counted, in particular with EPC, which is in agreement with the results of Mayer et al. (1985).

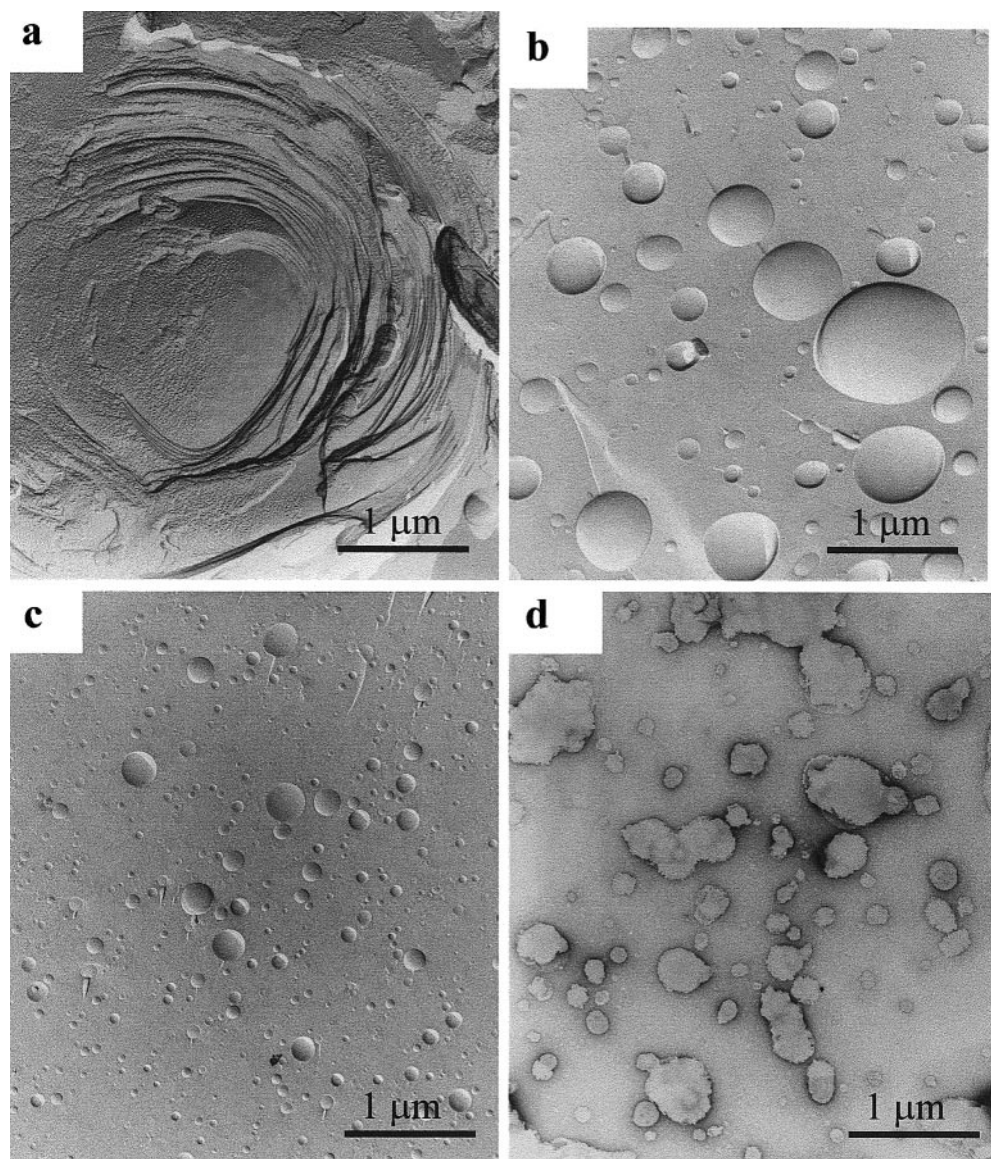
Dimensions of the unilamellar vesicles were determined from the fractured vesicles after 10 freeze-thaw cycles (see Materials and methods). Typical histograms of the percentage of vesicles of various diameters are shown in Fig. 2 for cases where efficient fragmentation took place. More than 40% of the counted vesicles had a diameter below 100 nm and the frequency decreased at greater diameters. The average diameter was reduced by the presence of DOPA, DOPG or LPC, suggesting a role of the charged lipids. Increasing the number of freeze-thaw cycles decreased the average vesicle size: after 50 cycles, more than 90% of counted vesicles had a diameter below 100 nm.

Note that if instead of histograms of the percentage of vesicles, histograms of the inner volume are represented for various values of D assuming spherical vesicles (Fig. 2), the same data (because of the factor D^3) reveal that the contribution of large or very large unilamellar vesicles (i.e. $D \geq 400$ nm) is in fact preponderant. Thus, in spite of the majority of very small vesicles, the entrapped volume per μmol of phospholipid is important with such liposome preparations. However, the fluctuations in the histograms representing the inner volumes (Fig. 2) emphasize the fact that the actual population of very large vesicles is difficult to establish in a statistically reliable fashion by electron microscopy, even when a population of several hundreds of unilamellar vesicles is examined. This is because these very large vesicles represent only a small percentage of the total population and, hence, counting only a few hundreds of vesicles is insufficient for good statistics.

Negative staining electron microscopy

This technique is often considered as more reliable for size determination. However, owing to the frequent overlap of vesicles on the grids and since the very small vesicles are difficult to visualize, the uncertainty may in fact be larger. Figure 1d, for example, shows vesicles with complicated shapes, which could be a superposition of several vesicles. Histograms have been made from

Fig. 1 Freeze-fracture electron micrographs (**a**, **b**, **c**) and negative staining (**d**) of aqueous dispersions of DOPC/DOPA (80:20 mol%) after: 0 (**a**); 10 (**b** and **d**) and 50 (**c**) cycles of freeze-thawing



negative staining data. The overall tendency was similar to that deduced from freeze-fracture experiments with, however, less very small vesicles (data not shown).

³¹P Broad band NMR and simulated spectra

Because of its sensitivity to the time scale of reorientation, ³¹P broad band NMR allows one to determine the distribution of vesicle sizes for vesicles with a diameter below 1 μm (Burnell et al. 1980). Figure 3 shows a set of theoretical NMR spectra corresponding to homogeneous populations of spherical phospholipid vesicles with diameters varying from 30 nm to 1 μm. Figure 4a–d shows experimental spectra obtained with a mixture of DOPC/DOPA (80:20 mol%) subjected to 0, 10, 20, and 50 freeze-thaw cycles, respectively. Figure 4e–h shows the corresponding simulated spectra.

The theoretical spectrum of Fig. 4e was obtained by assuming MLVs with an onion structure, i.e. assuming the superposition of vesicles stacked like Russian dolls with a continuous distribution from very large to very small vesicles (Douliez et al. 1994). However, the experimental spectrum corresponding to DOPC/DOPA mixtures (Fig. 4a) shows features which probably reflect the existence of a large proportion of vesicles with sub-micron diameters, possibly due to vesicles enriched in DOPA, hence reflecting improper mixing between DOPC and DOPA. Another possibility is that these DOPA containing vesicles have an ellipsoidal shape and hence are partially oriented in the magnetic field (Pott and Dufourc 1995). MLVs made of pure DOPC gave a more classical “bilayer type” spectrum (not shown).

When several freeze-thaw cycles are applied to this mixture, the overall NMR lineshapes reveal a decrease of the average vesicle size. It also demonstrates the

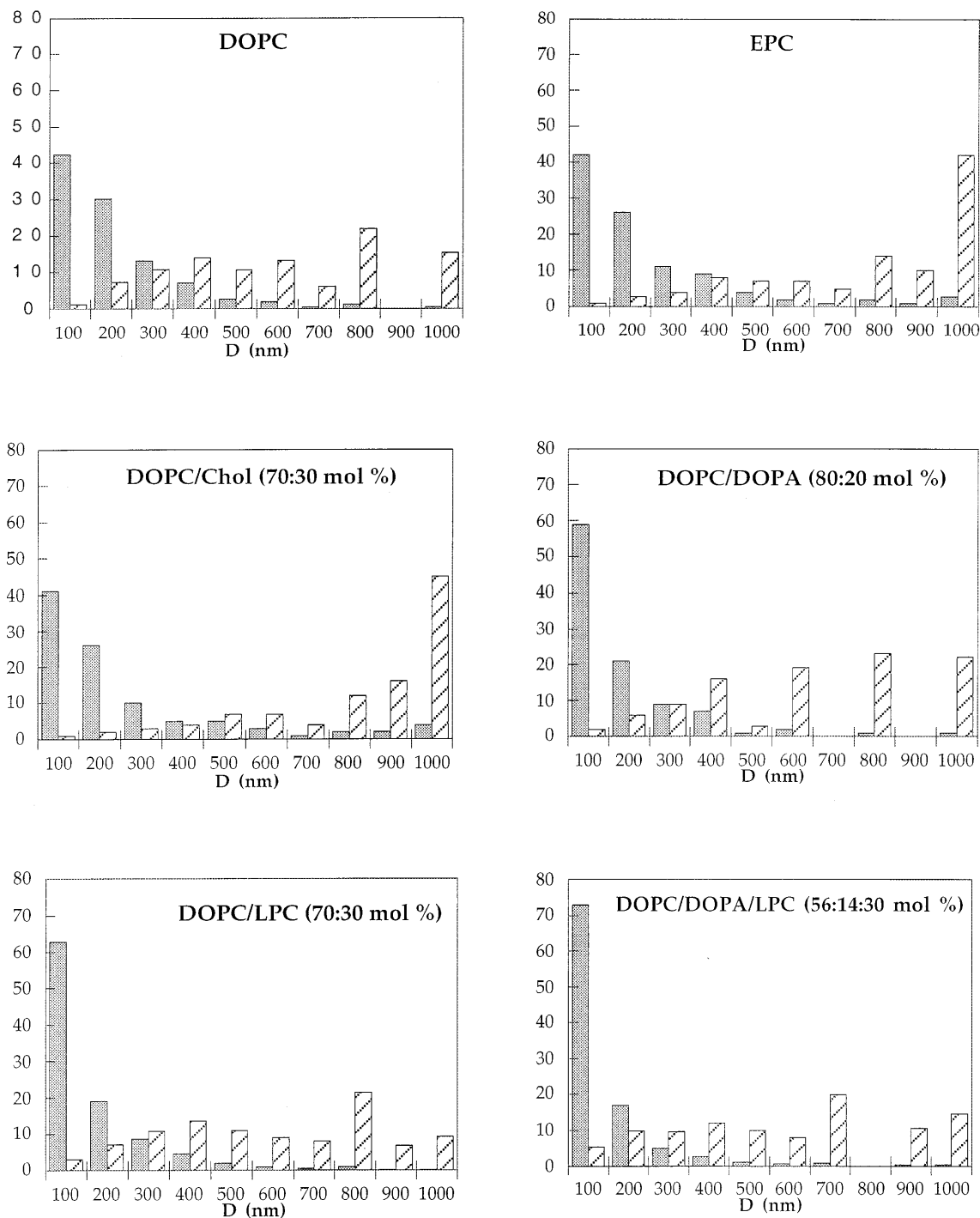


Fig. 2 Histograms indicating the percentage of vesicles of various diameters counted on freeze-fracture electron micrographs after 10 freeze-thaw cycles (*in gray*); the same figure shows the corresponding histograms indicating the percentage of vesicles contributing to the total entrapped volume assuming spherical vesicles (*hatched symbols*)

heterogeneity of vesicle sizes obtained by freeze-thawing. The narrow peak around 0 ppm corresponds to the presence of small vesicles for which the anisotropy of the chemical shift tensor is averaged out. The amplitude of this peak increases with the number of cycles (compare Fig. 4a and Fig. 4d). The overall lineshape may be

misleading because one sees only the two extreme spectral components associated with very large vesicles and very small vesicles, respectively. In reality, there is a continuous distribution of vesicle sizes. We have carried out a series of spectral simulations to determine the most likely distribution in the case of: (1) a lipid dispersion composed either of DOPC or DOPC/DOPA (80:20 mol%) with an increasing number of cycles, and (2) various lipid mixtures after 10 freeze-thaw cycles.

Several types of size distribution were tested and within each type of profile we varied the parameters to

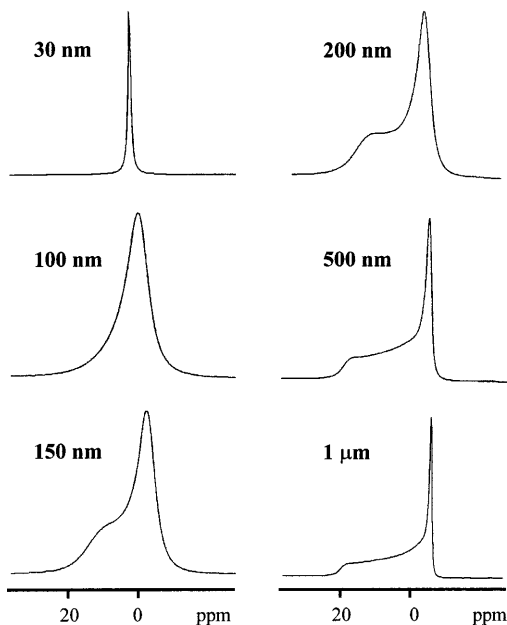


Fig. 3 Theoretical ^{31}P NMR spectra for homogeneous populations of unilamellar vesicles of different diameters

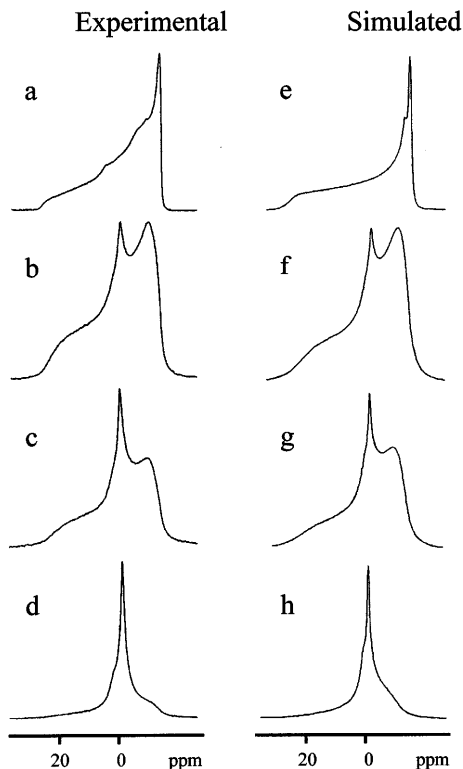


Fig. 4a-h Comparison between experimental and simulated ^{31}P NMR spectra for DOPC/DOPA (80:20 mol%). Number of freeze-thaw cycles: 0 (**a** and **e**); 10 (**b** and **f**); 20 (**c** and **g**); 50 (**d** and **h**). Theoretical spectra **f**, **g** and **h** were obtained with a distribution of vesicle diameters following an exponentially decreasing function. The average diameters \bar{D} of the exponential distributions were 98, 85 and 60 nm, respectively

optimize the matching between experimental and simulated spectra by comparing the integrals for spectra plotted with the same maximum intensity. The following type of distributions were used:

- Distributions corresponding to an exponentially decreasing function starting at D_0 with a characteristic length D_c .
- Half-Gaussian distributions starting at D_0 , with characteristic width D_c .
- Gaussian distributions with characteristic width D_c , centered at a finite average diameter \bar{D} .
- Distributions decreasing as $1/D^2$, limited to an interval between D_0 and D_{\max} .

In all cases, the minimum diameter D_0 was set at 30 nm. This is somewhat artificial because in reality there is no reason a priori to impose a cut-off at D_0 . However, this procedure is justified by the fact that NMR spectra in any case would not be sensitive to small variations of vesicle diameters below this minimum value D_0 . On the other hand, this method is very sensitive in the hundred nanometer diameter range, which makes it well suited for the present study.

Computer simulations showed that Gaussian distributions around a finite average diameter \bar{D} never permit a good fit of the experimental spectra (except in the case of LUVs), neither does a half-Gaussian distribution. Figure 5a-d shows various attempts to simulate the experimental spectrum of DOPC/DOPA mixtures after 20 freeze-thaw cycles using an exponential, a half-Gaussian and a Gaussian function, respectively. Best fits were obtained with the exponential probability function decreasing from D_0 . We found that reasonable fits could be obtained also with a probability decreasing as $1/D^2$ (data not shown). In the latter case an upper limit D_{\max} had to be set for normalization. However, there is no physical argument to justify a discontinuous probability for large diameters. The exponential frequency function, on the other hand, can be extended to infinity; the normalization is accounted for by the parameter D_c that is related to the average diameter by the following relation: $\bar{D} = D_c + D_0$.

In summary, the exponential probability function with a single parameter D_c permitted the best simulations of the NMR spectra recorded after freeze-thawing (Fig. 4b-d). Data summarizing \bar{D} values obtained for different lipid compositions are included in Table 1 together with mean vesicle diameters deduced from electron microscopy. There is a systematic difference between the average diameters deduced from electron microscopy and those deduced from NMR. Attempts to explain this discrepancy will be presented in the Discussion section.

Influence of cholesterol

The change in lineshape of ^{31}P NMR spectra recorded with DOPC/cholesterol mixtures (7/1 mol ratio) after 0,

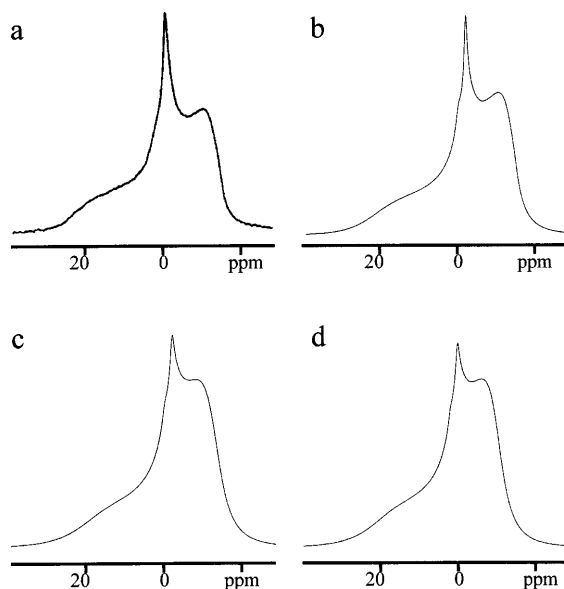


Fig. 5 Comparison between an experimental spectrum obtained after 20 cycles of freeze-thawing (spectrum **a**) and simulated spectra with various distributions of vesicle sizes: **b** exponentially decreasing function with $\bar{D} = 85$ nm; **c**, half-Gaussian profile, starting at $D_0 = 30$ nm with $D_c = 140$ nm; **d** Gaussian profile centered at $\bar{D} = 265$ nm, with a Gaussian width of 110 nm. The spectra are plotted with the same maximum amplitude. Calculation of their integral indicates that if spectrum **a** corresponds to $I_a = 1$, then: $I_b = 1.023$; $I_c = 1.115$; $I_d = 1.082$. For the simulations, T_2 was calculated with $R_1 = 20$ Hz and 500 Hz for DOPC and DPA, respectively. R_2 was fixed at 600 Hz. Changing arbitrarily R_1 and R_2 values in order to broaden or to narrow the lines did not allow a better fit in the case of a Gaussian or a semi-Gaussian distribution of vesicle sizes

Table 1 Average diameters of unilamellar vesicles obtained after 10 freeze-thaw cycles of aqueous dispersions

Lipids ^a	\bar{D} from NMR ^b	\bar{D} from Electron microscopy ^c
DOPC	110	167 (213)
DOPC/DOPA (80:20 mol%)	98	164 (210)
DOPC/DOPA (80:20 mol%) ^d	60	59 (76)
DOPC/DOPA (70:30 mol%)	88	–
DOPC/LPC (70:30 mol%)	–	125 (160)
DOPC/DOPA/LPC (72:18:10 mol%)	80	108 (138)
DOPC/DOPA/LPC (56:14:30 mol%)	75	100 (128)
DOPC/DOPG (70:30 mol%)	75	–
DOPC/Chol (70:30 mol%)	160	216 (276)
EPC	105	207 (265)
POPC	130	–

^a Lipids were dispersed in pH 8 buffer

^b Average diameter, $\bar{D} = D_0 + D_c$ (in nm), deduced from simulation using an exponential probability function. A variation of \bar{D} of the order of ± 2 nm suffices to modify the lineshape, indicating that the precision obtained for this parameter from the simulations is high. On the other hand, this does not prove the uniqueness of the model to fit the data

^c Average diameter \bar{D} (in nm), obtained directly on the freeze-fracture electron micrographs. In parentheses is the value including the correcting factor (see text)

^d 50 freeze-thaw cycles

1 or 10 freeze-thaw cycles (Fig. 6) confirms electron microscopy observations (Fig. 2) which showed the fragmentation of DOPC/cholesterol vesicles. NMR confirms also that average diameters remain much larger than in the case of DOPC or DOPC/DOPA vesicles (see Table 1).

Lipid mixtures that do not fragment

Freeze-fracture electron microscopy was also carried out with freeze-thawed suspensions of DMPC, DPPC, ESM or DLnPC. In contrast to the previous mixtures, the latter lipid suspensions remained essentially multilamellar even after 10 cycles. Electron microscopy as well as ^{31}P NMR carried out with these lipids revealed at once that they do not fragment into small vesicles during the process of freeze-thawing, at least under our experimental conditions. In the case of DMPC/DMPA or DOPC with more than 30% cholesterol, NMR spectra obtained after 10 cycles indicated partial fragmentation. Figure 7 shows micrographs from freeze-fracture electron microscopy and NMR spectra of some of these lipids after 10 cycles of freeze-thawing. The lineshape obtained with ESM before freeze-thawing suggests partial orientation of the MLVs owing to the magnetic field as reported already by several investigators (Brumm et al. 1992; 1995; Picard et al. 1999; Pott and Dufourc, Seelig et al. 1985).

Large unilamellar vesicles

Repetitive freeze-thawing was also successful in reducing the diameter of LUVs with an initial diameter of the order of 200 nm as obtained by reverse phase evaporation. If freeze-thawing was carried out with LUVs in buffer, NMR spectroscopy indicated a narrowing of the ^{31}P NMR spectrum (Fig. 8). Importantly, simulation of

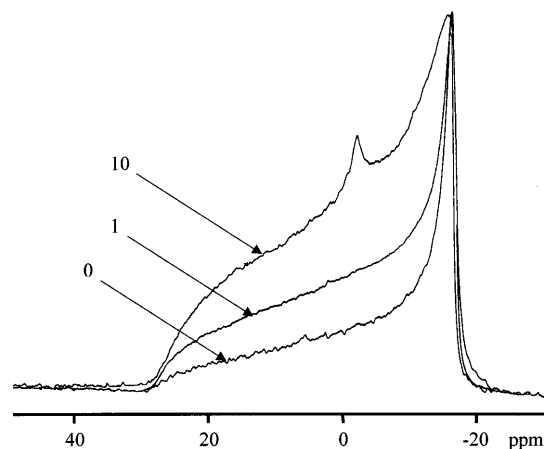


Fig. 6 Evolution of the ^{31}P NMR spectrum obtained with an aqueous dispersion of DOPC/cholesterol (70:30 mol%) after 0, 1 and 10 cycles of freeze-thawing, respectively

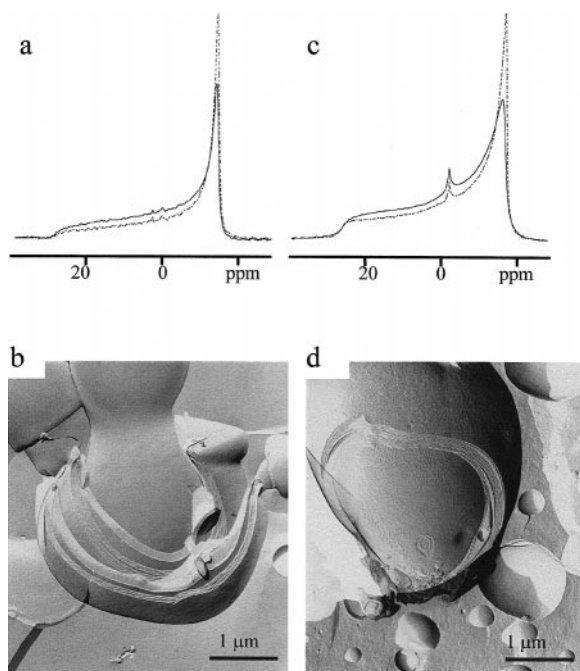


Fig. 7a–d ^{31}P NMR spectra and freeze-fracture electron micrographs of aqueous dispersions of lipids that do not fragment or only partially fragment after 10 cycles of freeze-thawing. **a** and **b**: ESM; **c** and **d**: DLnPC. **a** and **c** show (dotted lines) the NMR spectra before freeze-thawing and (full line) the spectra after 10 cycles. The freeze-fracture micrographs were obtained after 10 cycles

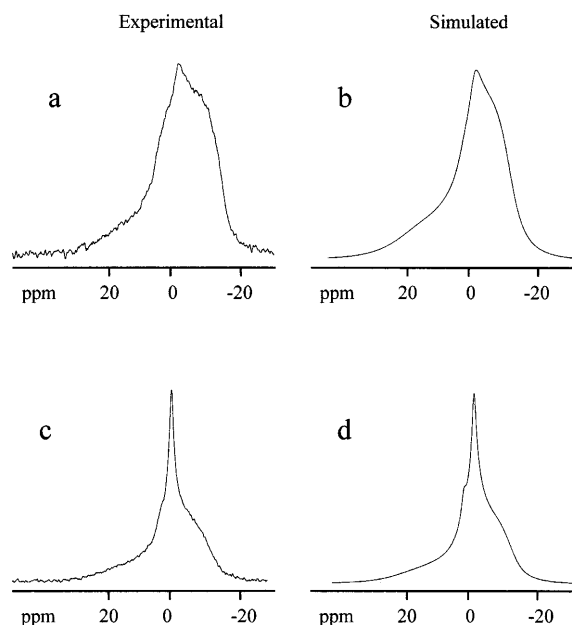


Fig. 8 Comparison between experimental (**a** and **c**) and simulated (**b** and **d**) ^{31}P NMR spectra of LUVs made of DOPC/DOPA (80:20 mol%). Spectrum **a** was obtained after extrusion of liposomes through 200 nm pores before freeze-thawing; spectrum **c** was obtained after 10 freeze-thaw cycles applied to the LUV suspension. The theoretical spectrum **b** was obtained by using a Gaussian distribution of vesicle diameters, centered at $\bar{D} = 225$ nm and a Gaussian width of 81 nm. Spectrum **d** was obtained with an exponentially decreasing distribution and $\bar{D} = 65$ nm. For more details, see text

the experimental spectrum corresponding to LUVs with diameters around 200 nm before freeze-thawing with a Gaussian distribution centered around 200 nm gave a good fit (Fig. 8a and b). On the other hand, the spectrum obtained after 10 cycles of freeze-thawing (Fig. 8c) is practically identical to that obtained after 50 cycles when starting with MLVs (Fig. 4h), suggesting that fragmentation of vesicles by freeze-thawing reaches a limit.

Sonicated vesicles

When sonicated vesicles were subjected to cycles of freeze-thawing, the ^{31}P NMR spectra were also modified and indicated the fusion and/or aggregation of at least a fraction of the vesicles. The efficiency of this process depended on the buffer: in pure water, after a single freeze-thaw cycle, sonicated DOPC SUVs appear to be heterogeneous with the coexistence of small vesicles and very large vesicles (Fig. 9d); after five cycles the small vesicles had disappeared, as indicated by the broad NMR spectrum (Fig. 9f). If SUVs of DOPC were made in salt containing buffer, only a small broadening of the narrow peak associated with SUVs took place (Fig. 9c and e). Similarly, SUVs made of DOPC/DOPA (80:20 mol%) gave rise to a small line broadening while with DOPC/DOPA/LPC (60:13:27) no detectable broadening was seen after 10 cycles (not shown). Electron microscopy (Fig. 9g and h) demonstrates also the influence of the buffer and seems to indicate that fusion happens rather than aggregation, in agreement with Pick's measurements of the trapping capacity of sonicated vesicles submitted to freeze-thawing (Pick 1981).

Discussion

Certain lipid mixtures containing unsaturated chains, when dispersed in buffer and subjected to cycles of freeze-thawing, form unilamellar vesicles as reported by Mac Donald et al. (1994). Here, we used liquid nitrogen for the cooling and a water bath at 60 °C for heating. We have deliberately tried a single temperature for cooling and limited ourselves to one buffer composition since an extensive study of the nature and concentration of electrolytes had been done previously by MacDonald et al. (1994). On the other hand, we have extended the assay to other lipid mixtures for which this protocol can be applied with success and we have quantified the unilamellarity and size distribution of the vesicles.

Electron microscopy as well as ^{31}P NMR indicated a range of heterogeneity of vesicle sizes after freeze-thawing. Both techniques showed that the proportion of vesicles of a given size can be represented by an exponentially decreasing function of the diameter, with a characteristic averaged diameter \bar{D} function of the number of cycles. However, we found a systematic difference between the average value determined from

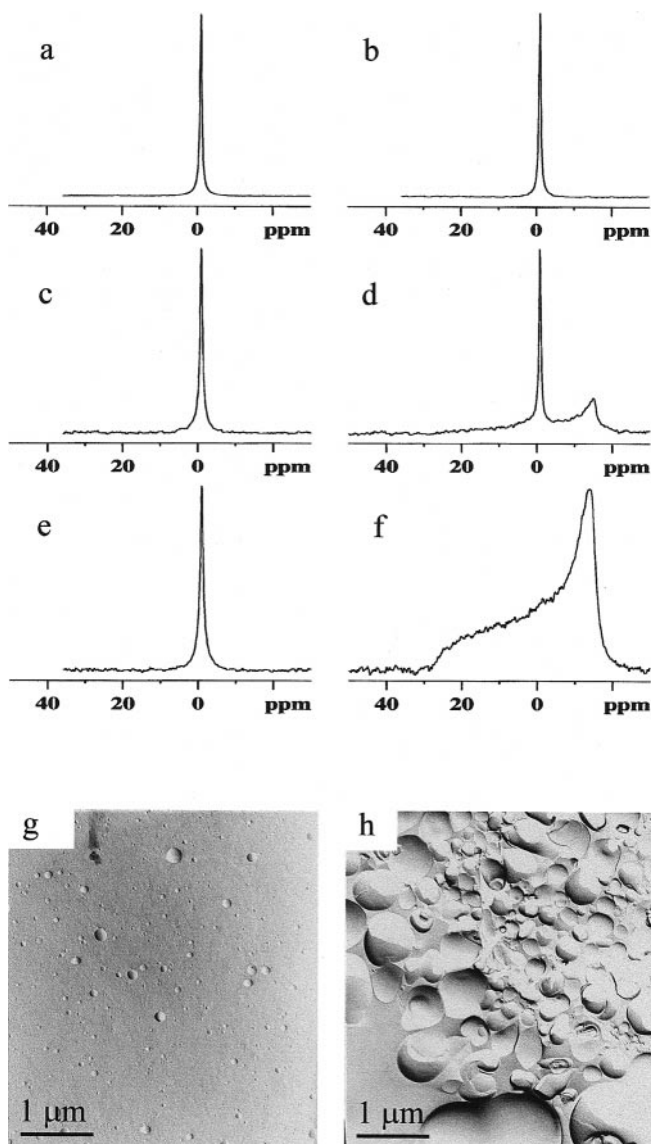


Fig. 9 ^{31}P NMR spectra and freeze-fracture electron micrographs of sonicated dispersions of DOPC with buffer (**a, c, e, g**) and in water (**b, d, f, h**). Number of freeze-thawing cycles: **a** and **b**, 0; **c** and **d**, 1; **e, f, g** and **h**, 5

NMR simulations and that deduced from electron microscopy. In the latter case, the average diameter was multiplied by a factor between 1.5 and 2. One control of the validity of NMR simulation is our ability to simulate the spectrum of LUVs obtained by phase reversion and filtration at 200 nm. The average diameter deduced from the simulation was indeed very close to 200 nm. Nevertheless, one may ask if an erroneous value of the diffusion rate constant utilized in other NMR simulations could explain the discrepancy with electron microscopy. In these calculations, we used $D_{\text{diff}} = 10^{-7} \text{ cm}^2/\text{s}$ which is the value proposed by Galla et al. (1979) for DOPC. When examining the data in the literature corresponding to the diffusion of phospholipids in the fluid phase around room temperature, values reported range from

1.3×10^{-7} to $10^{-8} \text{ cm}^2/\text{s}$ (Blume 1993; Devaux and McConnell 1972). If a lower diffusion constant was used (say $0.5 \times 10^{-7} \text{ cm}^2/\text{s}$), it would be necessary to reduce the average diameter \bar{D} in the simulation. Indeed, slower diffusion imposes smaller vesicles in order to obtain the same reorientation rate. Similarly, if the water viscosity is increased artificially in the calculation to take into account the high concentration of vesicles, the orientation averaging becomes less efficient unless the average diameters are again reduced. Thus, in both instances the discrepancy between NMR and electron microscopy is aggravated.

In the case of NMR, small vesicles contribute very significantly to the lineshape, owing to the fact that they give narrow and therefore intense peaks. Large vesicles also contribute to the spectral intensity owing to the large number of lipids in each vesicle. The latter contribution is in a different region of the spectrum. More important, owing to the low sensitivity of NMR, a single spectrum corresponds to the averaging of a very large number of vesicles, exceeding by several orders of magnitude the number of vesicles that can be reasonably counted from electron micrographs.

A difficulty with electron microscopy is that vesicles may not be counted on a single micrograph if their diameters vary considerably, as is frequently the case. Indeed, large vesicles can be counted easily but it is difficult, if not impossible, to count very small vesicles on the same micrograph (i.e. with the same magnification). Yet micrographs contain vesicles with diameters varying from 30 nm to almost 1 μm . Thus, an underestimation of the number of small vesicles that are counted on electron micrographs is highly probable.

Another problem is the actual vesicle shapes. The correcting factor 1.28 which is applied to the size measurements in Table 1 (values between parentheses in the third column) is only valid for perfect spheres (Heegaard et al. 1990). Indeed, freeze-fracture electron microscopy shows essentially spherical objects. However, negative staining shows vesicles with more complicated shapes. (Fig. 1d). It is possible that glycerol is responsible for the sphericity of vesicles seen by freeze-fracture electron microscopy. Recently, we have observed LUVs by cryoelectron microscopy in the absence or presence of glycerol. It appears that while vesicles are all spherical in the presence of glycerol, in the absence of glycerol their shape can be discoid, elongated or invaginated (Traïkia M, Lambert O, Rigaud J-L, Devaux PF, in preparation). If the vesicles which are used for NMR in the absence of glycerol have surfaces covered with invaginations and protrusions, then the orientation averaging will be much faster than with perfect spheres. Certain vesicles may have an ellipsoidal deformation. The NMR spectra in Fig. 7 and perhaps spectrum a in Fig. 4 have features indicative of a partial orientation of the vesicles in the magnetic field. Such magnetic orientation due to the anisotropy of the lipid diamagnetism can happen in the case of ellipsoidal deformation of the lipid vesicles (Pott and Dufourc 1995). Thus, the non-sphericity of the lipid

vesicles could explain, at least partially, why NMR gives smaller \bar{D} values than electron microscopy.

In conclusion, both techniques have their limitations at a quantitative level. However, they both indicate the same trend: namely, that the unilamellar vesicle sizes are not identical, the majority of the vesicles have a small diameter and the average diameter is reduced as the number of freeze-thaw cycles is increased. Table 1 indicates that after 10 freeze-thawing cycles the "average" vesicle size is comparable to that of LUVs obtained by filtration with an extruder. However, a large fraction of the vesicles have a much smaller diameter. Filtration of freeze-thawed vesicles will eliminate the very large vesicles remaining, but filtration will not permit one to obtain a homogeneous population of vesicles. Thus, in spite of its simplicity, the advantage of this technique for the production of unilamellar vesicles might be questioned if one needs a population of vesicles perfectly homogeneous in size. On the other hand, an advantage of the freeze-thaw technique is that it is not impeded by the presence of charged lipids, unlike the extruder technique (unpublished results from our laboratory).

Is it possible to predict the efficiency of freeze-thawing for a given lipid composition and one can explain the mechanism of fragmentation? As revealed by freeze-fracture electron microscopy, MLVs fragmentation into small unilamellar vesicles takes place progressively: a homogeneous population of unilamellar vesicles requires between five and ten cycles of freeze-thawing. Although we have not attempted a systematic investigation of the minimum number of cycles for each lipid composition used in these experiments, it is apparent that pure DOPC fragments faster than DOPC/cholesterol mixtures. For concentrations of cholesterol above 30%, fragmentation was not observed. However, there is an upper limit on the cholesterol concentration that can be accommodated within the bilayer structure and this limit strongly depends on the sample preparation procedure (Huang et al. 1999). Excess cholesterol will precipitate as crystals of pure cholesterol monohydrate and could perturb light absorbance measurements. This observation may explain the difference between our results and those of MacDonald et al. concerning the DOPC/Chol mixtures. At any rate, membrane fluidity appears to be important for this process to take place: DMPC, DPPC and ESM, all lipids that do not fragment, are in a gel phase at the temperature of ice formation; by contrast DOPC, POPC and EPC, lipids that do fragment, are fluid at that temperature. However, as pointed out already by MacDonald et al., the fact that membranes are fluid or rigid when ice forms is not a definitive criteria since DLnPC, which is a lipid with double bonds and a transition temperature below 0 °C, does not fragment (see Fig. 7). Because fragmentation takes place only in the presence of salt, it is likely, as pointed out by previous investigators, that osmotic effects are involved. Membrane breakage by osmotic shocks will be favored by the inhomogeneous distribution of ions in MLVs (Gruner et al. 1985), the entrapped buffer exhibiting reduced

solute concentrations. It is noteworthy that very small vesicles like SUVs are resistant to osmotic shocks; thus vesicles that do fragment seem to reach progressively a state where the surface tension associated with high curvature is a maximum.

Acknowledgements The authors thank Dr. Erick J. Dufourc for allowing us to use his simulation program. We also thank Dr. Richard Callaghan for critically reading the manuscript.

References

- Blume A (1993) Dynamic properties. In: Cevec G (ed) *Phospholipids handbook*. Dekker, New York, pp 555–509
- Brumm T, Möps A, Dolainsky C, Bayerl TM (1992) Macroscopic orientation effects in broad line NMR spectra of model membranes at high magnetic field strength. A method for preventing such effects. *Biophys J* 61: 1018–1024
- Burnell EE, Cullis PR, De Kruijff B (1980) Effects of tumbling and lateral diffusion on phosphatidylcholine model membrane ^{31}P -NMR lineshapes. *Biochim Biophys Acta* 603: 63–69
- Devaux P, McConnell HM (1972) Lateral diffusion in spin labeled phosphatidylcholine-multilayers. *J Am Chem Soc* 94: 4475–4481
- Doulez JP, Bellocq AM, Dufourc EJ (1994) Effect of vesicle size, polydispersity and multilayering on solid state ^{31}P - and ^2H -NMR spectra. *J Chem Phys* 91: 874–880
- Dufourc EJ, Mayer C, Strorer J, Althoff G, Kothe G (1992) Dynamics of phosphate head groups in biomembranes. A comprehensive analysis using phosphorus-31 nuclear magnetic resonance lineshape and relaxation measurements. *Biophys J* 61: 42–57
- Galla H-J, Hartmann W, Theilen U, Sackmann E (1979) On two-dimensional passive random walk in lipid bilayers and fluid pathways in biomembranes *J Membr Biol* 48: 215–236
- Gruner SM, Lenk RP, Janoff AS, Ostro MJ (1985) Novel multilayered lipid vesicles: comparison of physical characteristics of multilamellar liposomes and stable plurilamellar vesicles. *Biochemistry* 24: 2833–2842
- Heegaard CW, Le Maire M, Gulik-Krzywicki T, Moller JV (1990) Monomeric states and Ca^{2+} transport by sarcoplasmic reticulum Ca^{2+} ATPase, reconstituted with an excess of phospholipid. *J Biol Chem* 265: 12020–12028
- Hope MJ, Bally MB, Webb G, Cullis PR (1985) Production of large unilamellar vesicles by rapid extrusion procedure. Characterization of size distribution, trapped volume and ability to maintain a membrane potential. *Biochim Biophys Acta* 812: 55–65
- Huang J, Buboltz JT, Feigenson GW (1999) Maximum solubility of cholesterol in phosphatidylcholine and phosphatidylethanolamine bilayers. *Biochim Biophys Acta* 1417: 89–100
- MacDonald RC, Jones FD, Qiu R (1994) Fragmentation into small vesicles of dioleoylphosphatidylcholine bilayers during freezing and thawing. *Biochim Biophys Acta* 1191: 362–370
- Mayer LD, Hope MJ, Cullis PR, Janoff AS (1985) Solute distributions and trapping efficiencies observed in freeze-thawed multilamellar vesicles. *Biochim Biophys Acta* 817: 193–196
- Oku N, MacDonald RC (1983) Differential effects of alkali metal chlorides on formation of giant liposomes by freezing and thawing and dialysis. *Biochemistry* 22: 855–863
- Picard F, Paquet MJ, Levesque J, Bélanger A, Auger M (1999) ^{31}P NMR first spectral moment study of the partial magnetic orientation of phospholipid membranes. *Biophys J* 77: 888–902
- Pick U (1981) Liposomes with a large trapping capacity prepared by freezing and thawing of sonicated phospholipid mixtures. *Arch Biochem Biophys* 212: 186–194

- Pott T, Dufourc EJ (1995) Action of melittin on the DPPC-cholesterol liquid-ordered phase: a solid state ^2H - and ^{31}P -NMR study. *Biophys J* 68: 965–977
- Rance M (1981) PhD thesis. University of Guelph, Canada
- Rance M, Byrd RA (1983) Obtaining high-fidelity spin-1/2 powder spectra in anisotropic media: phase cycled Hahn echo spectroscopy. *J Magn Res* 52: 221–240
- Roux M, Huynh-Dinh T, Igolen J, Prigent Y (1983) Simple preparation of 1,2-dipalmitoyl-*sn*-glycero-3-phosphoric acid and deuterated choline derivatives. *Chem Phys Lipids* 33: 41–45
- Seelig J (1978) ^{31}P nuclear magnetic resonance and head group structure of phospholipids in membranes. *Biochim Biophys Acta* 515: 105–140
- Seelig J, Borle F, Cross TA (1985) Magnetic ordering of phospholipid membranes *Biochim Biophys Acta* 814: 195–198
- Smith ICP, Ekiel IH (1984) Phosphorus-31 NMR of phospholipids in membranes. In: Gorenstern D (ed) *Phosphorus-31 NMR. Principles and applications*. Academic Press, New York, p 447
- Swairjo MA, Seaton BA, Roberts MF (1994) Effect of vesicle composition and curvature on the dissociation of phosphatidic acid in small unilamellar vesicles: a ^{31}P -NMR study. *Biochim Biophys Acta* 1191: 354–361
- Szoka FC, Olson F, Heath T, Vail WJ, Mayhew E, Papahadjopoulos D (1980) Preparation of unilamellar liposomes of intermediate size (0.1–0.2 microns) by a combination of reverse phase evaporation and extrusion through polycarbonate membranes. *Biochim Biophys Acta* 601: 559–571
- Traïkia M, Langlais DB, Cannarozzi, GM, Devaux PF (1997) High resolution spectra of liposomes using MAS NMR. The case of intermediate size vesicles. *J Magn Res* 125: 140–144